

# Supporting Information

## Selenium-Rich Nickel Cobalt Bimetallic Selenide with Core-Shell Architecture Enables Superior Hybrid Energy Storage Device

Yi-Lin Liu<sup>a,1</sup>, Cheng Yan<sup>a,b,1</sup>, Gui-Gen Wang<sup>a,\*</sup>, Fei Li<sup>a</sup>, Qi Kang<sup>c</sup>, Hua-Yu Zhang<sup>a,\*</sup>,

Jie-Cai Han<sup>a,d</sup>

<sup>a</sup>*Shenzhen Key Laboratory for Advanced Materials,*

*Harbin Institute of Technology, Shenzhen, Shenzhen 518055, China*

<sup>b</sup>*School of Chemistry, Faculty of Science, The University of Sydney, Sydney, New South Wales 2006, Australia*

<sup>c</sup>*Department of Polymer Science and Engineering, Shanghai Key Laboratory of Electrical Insulation and Thermal Ageing, Shanghai Jiao Tong University, Shanghai 200240, China*

<sup>d</sup>*Center for Composite Materials, Harbin Institute of Technology, Harbin 150080, China*

**KEYWORDS:** *nickel cobalt selenide, cathode, energy storage, core-shell structure, battery-supercapacitor hybrids*

E-mail: wangguigen@hit.edu.cn (Gui-Gen Wang)  
E-mail: hyzhang@hit.edu.cn (Hua-Yu zhang)

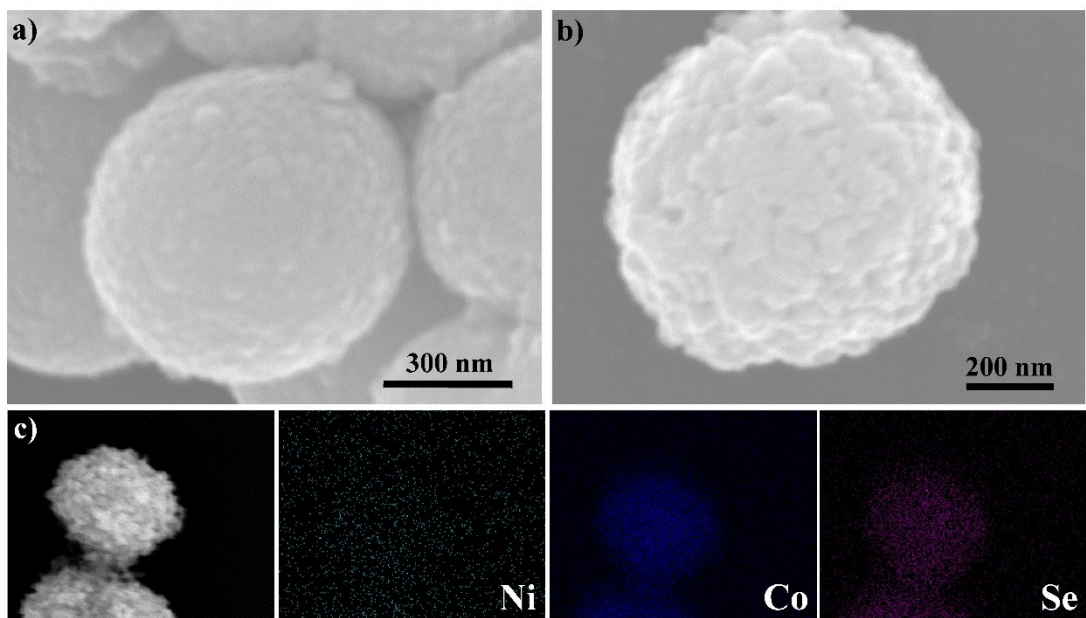


**Figure S1.** SEM images of the  $\text{Co}_9\text{Se}_8/\text{Co}_{0.85}\text{Se}-1$  at a) and b) low magnification; c) The corresponding EDS elemental mappings of Ni, Co and Se.

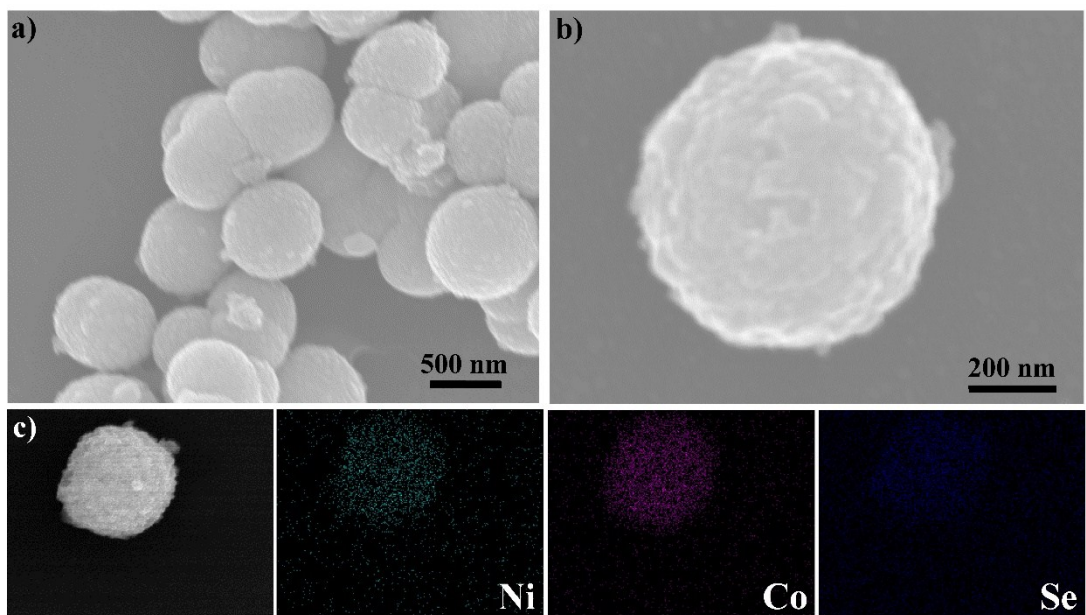


**Figure S2.** SEM images of the  $(\text{NiCo})_9\text{Se}_8/(\text{NiCo})_{0.85}\text{Se}-0.5$  at a) and b) low magnification; c) The corresponding EDS elemental mappings of Ni, Co and Se.

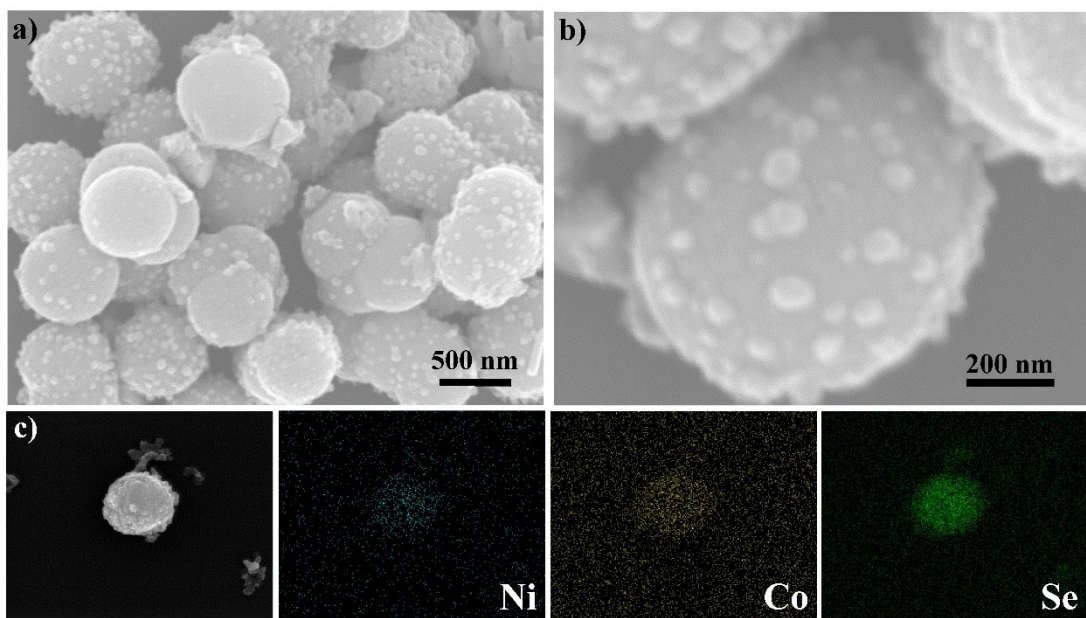


**Figure S3.** SEM images of the  $(\text{NiCo})_9\text{Se}_8/(\text{NiCo})_{0.85}\text{Se}-2$  at a) and b) low magnification; c) The corresponding EDS elemental mappings of Ni, Co and Se.

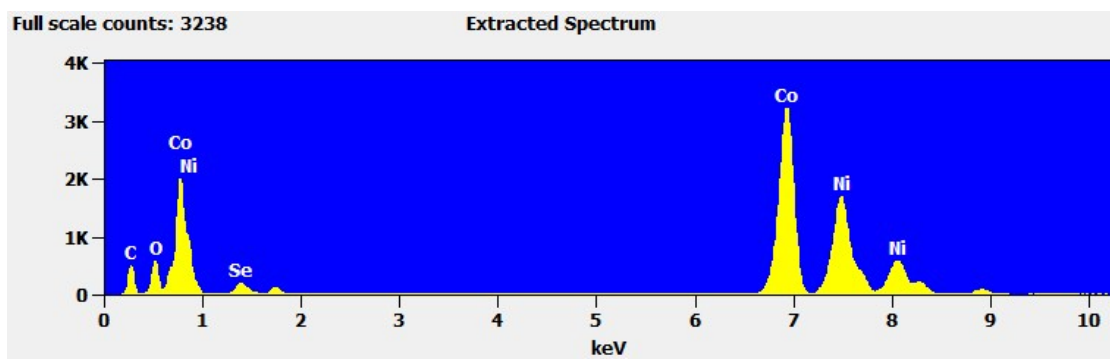


**Figure S4.** The EDS spectrum of the  $(\text{NiCo})_9\text{Se}_8/(\text{NiCo})_{0.85}\text{Se}-1$  core-shell sphere.

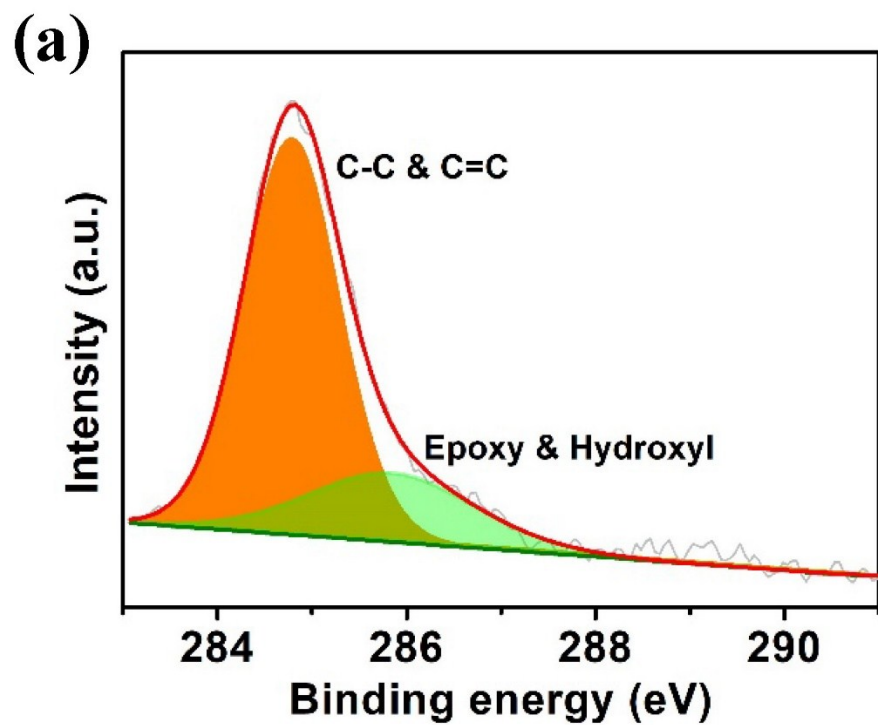


**Figure S5.** XPS spectra of the as-synthesized  $(\text{NiCo})_9\text{Se}_8/(\text{NiCo})_{0.85}\text{Se}-1$  core-shell sphere: C 1s.

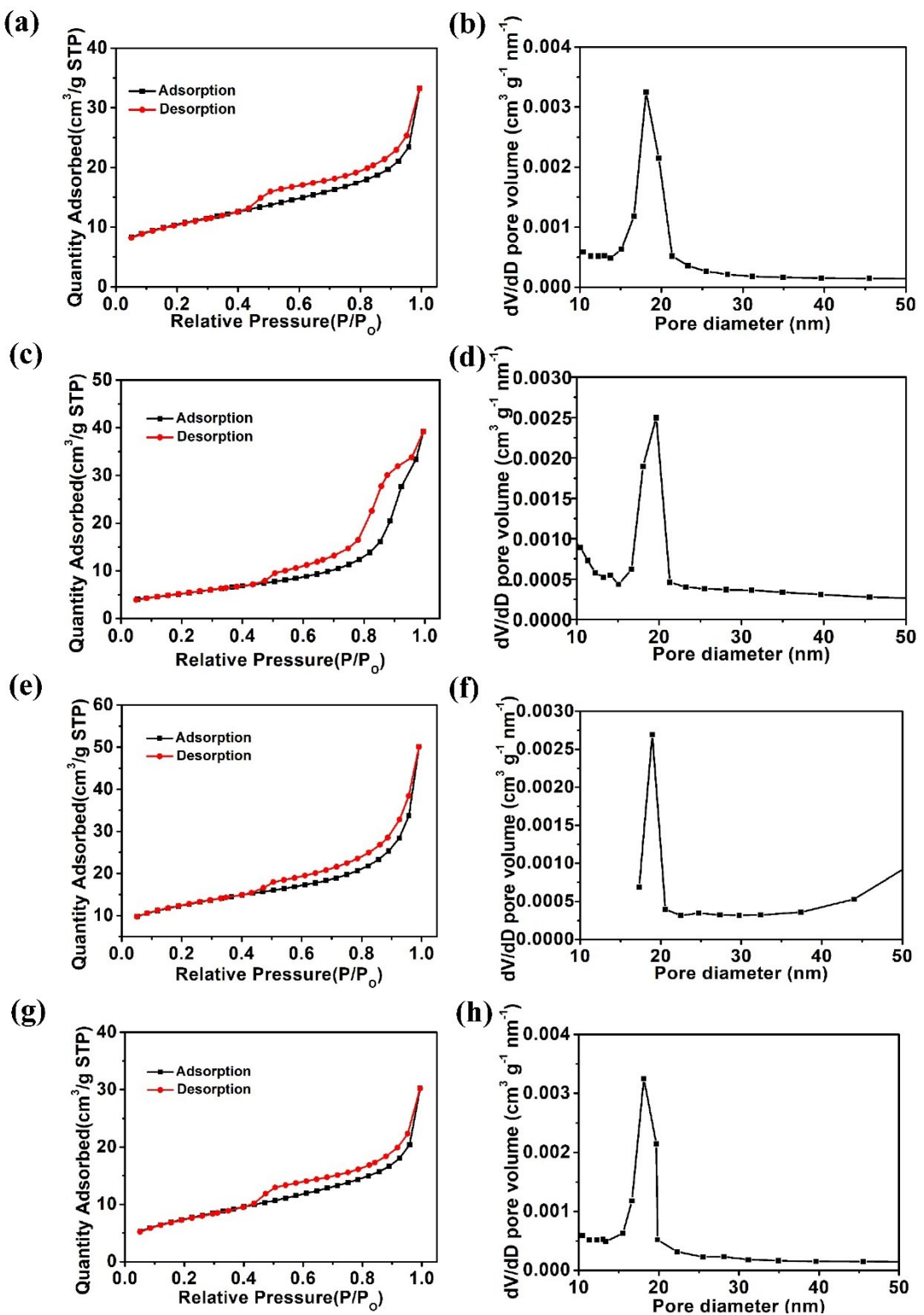


**Figure S6.** BET test: Nitrogen adsorption/desorption isotherms and the pore-size

distribution. a-b) Co<sub>9</sub>Se<sub>8</sub>/Co<sub>0.85</sub>Se-1; c-d) (NiCo)<sub>9</sub>Se<sub>8</sub>/(NiCo)<sub>0.85</sub>Se-0.5; e-f)

(NiCo)<sub>9</sub>Se<sub>8</sub>/(NiCo)<sub>0.85</sub>Se-1; g-h) (NiCo)<sub>9</sub>Se<sub>8</sub>/(NiCo)<sub>0.85</sub>Se-2.

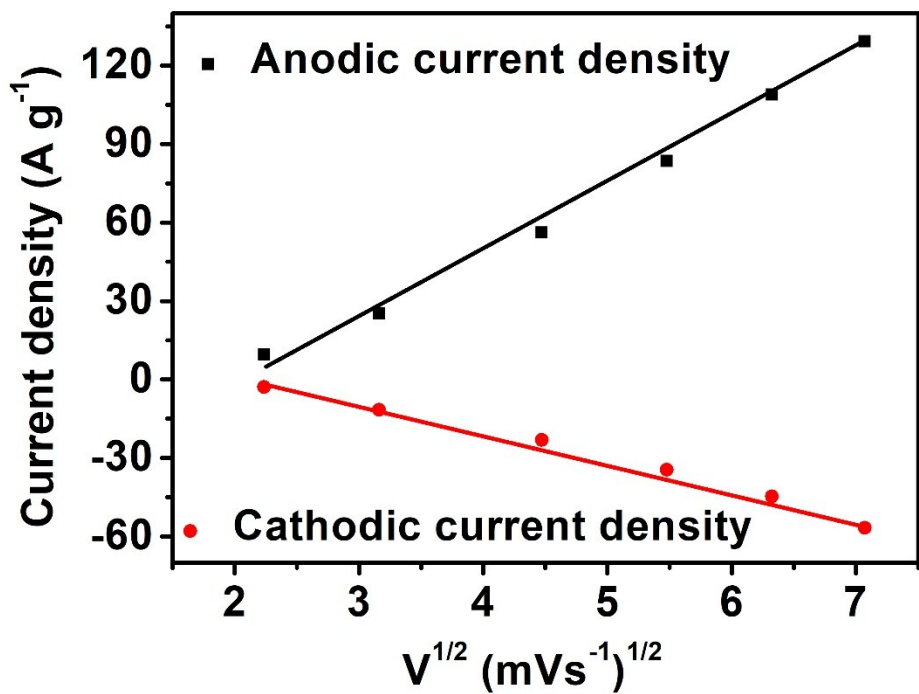
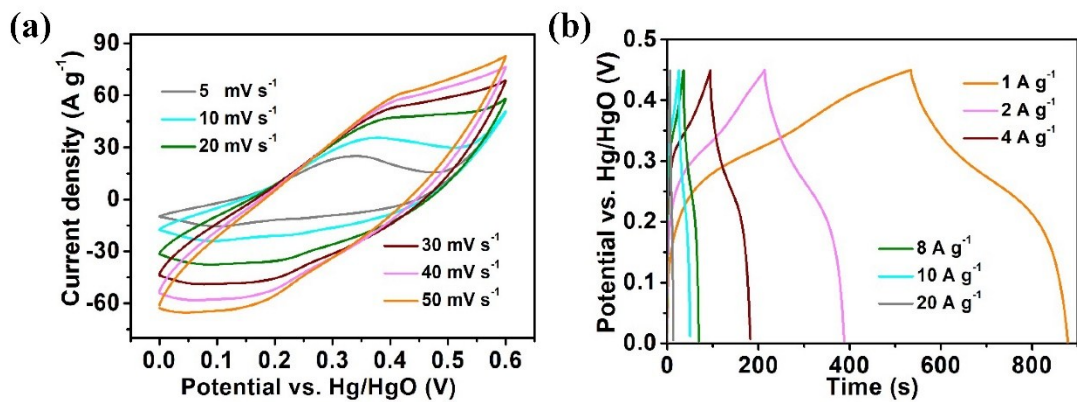
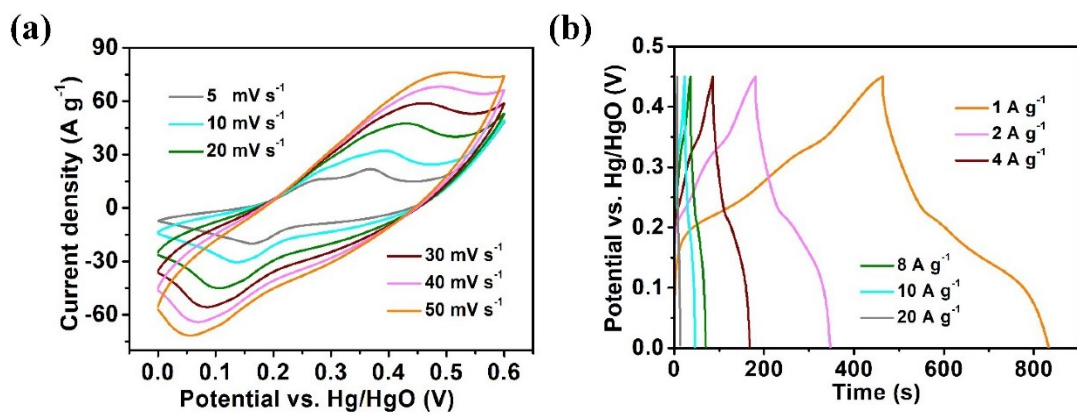


Figure S7. Correlation between peak current density and square roots of scan rates of Ni-Co-Se-1

Ni-Co-Se-1



**Figure S8.** The electrochemical performance of the  $\text{Co}_9\text{Se}_8/\text{Co}_{0.85}\text{Se}-1$ : (a) The CV curves; (b) The GCD curves.



**Figure S9.** The electrochemical performance of the  $(\text{NiCo})_9\text{Se}_8/(\text{NiCo})_{0.85}\text{Se}-0.5$ : (a) The CV curves; (b) The GCD curves.

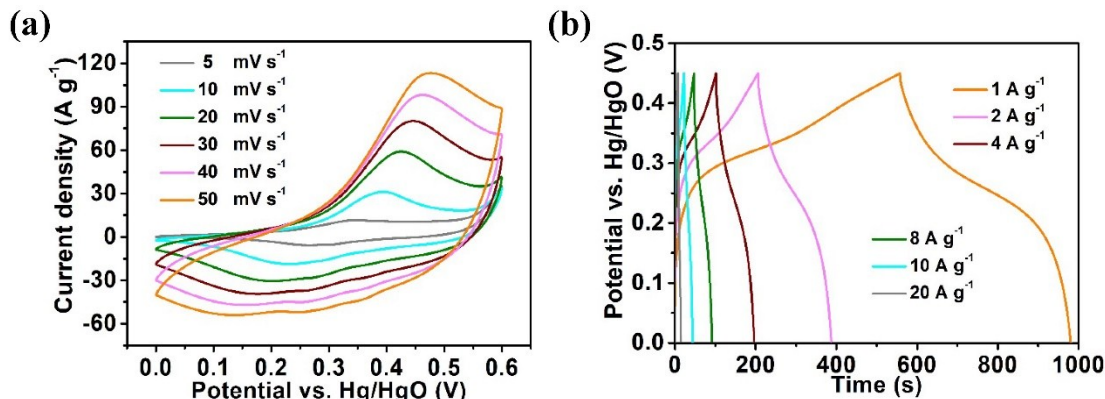


**Figure S10.** The electrochemical performance of the  $(\text{NiCo})_9\text{Se}_8/(\text{NiCo})_{0.85}\text{Se}-2$ : (a) The CV curves; (b) The GCD curves.

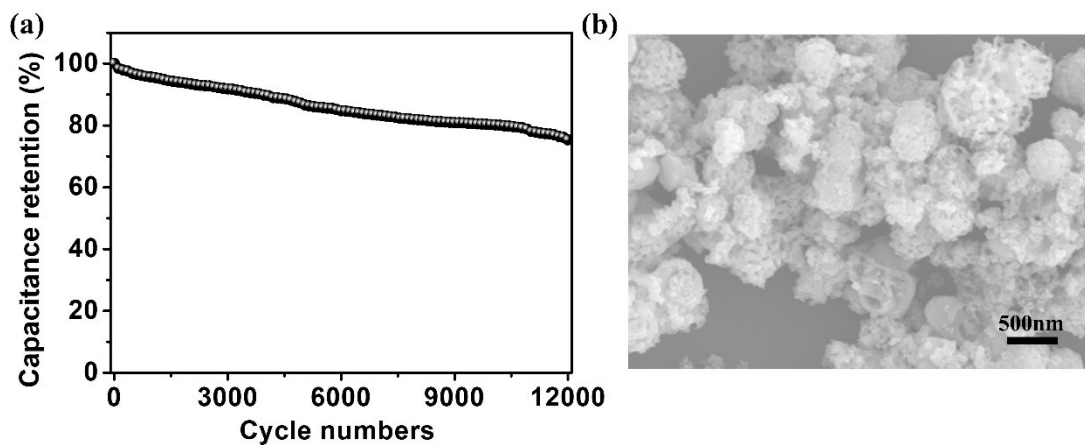


**Figure S11.** Electrochemical properties of the Ni-Co-Se-1: (a) The cycling performance; (b) SEM images of Ni-Co-Se-1 after 12000 cycles.

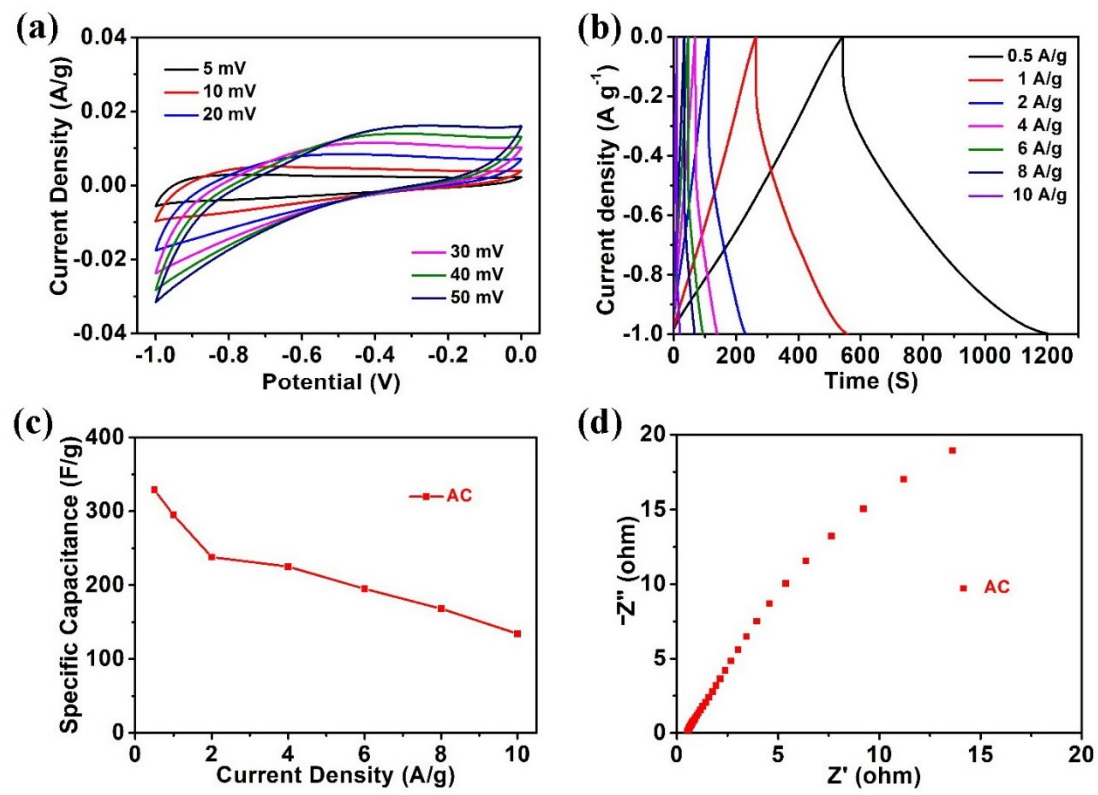


**Figure S12.** The electrochemical performance of AC: (a) The CV curves; (b) The GCD curves; (c) Rate performance; (d) EIS curves.

**Table S1.** Comparison of electrochemical performance between various hybrid pseudocapacitive electrodes and our work.

Electrode composition	Electrolyt	Specific capacitance		Counter electrode	Cyclic stability	Ref.
		e				
(NiCo) <sub>9</sub> Se <sub>8</sub> / (NiCo) <sub>0.85</sub> Se	1M KOH	164.44 mAh g <sup>-1</sup> at 1 A g <sup>-1</sup> (1315.52 F g <sup>-1</sup> at 1 A g <sup>-1</sup> / 591 C g <sup>-1</sup> at 1 A g <sup>-1</sup> )		Hg/HgO electrode	85.72 % after 5000 cycles	This work
Ni <sub>0.67</sub> Co <sub>0.33</sub> Se <sup>[1]</sup>	6M KOH	535 C g <sup>-1</sup> at 1 A g <sup>-1</sup>		Hg/HgO electrode	63 % after 2000 cycles	S1
NiSe-CoSe <sup>[2]</sup>	6M KOH	584 C g <sup>-1</sup> at 1 A g <sup>-1</sup>		Hg/HgO electrode	83.8 % after 1000 cycles	S2
(Ni <sub>0.33</sub> Co <sub>0.67</sub> )Se <sub>2</sub> <sup>[3]</sup>	3M KOH	827.9 F g <sup>-1</sup> at 1 A g <sup>-1</sup>		saturated calomel electrode	78.1 % after 2000 cycles	S3
Co <sub>0.85</sub> Se nanosheet <sup>[4]</sup>	2M KOH	422 F g <sup>-1</sup> at 1 A g <sup>-1</sup>		saturated calomel electrode	93 % after 2000 cycles	S4
NiCoSe <sub>2</sub> <sup>[5]</sup>	6M KOH	750 F g <sup>-1</sup> at 3 A g <sup>-1</sup>		saturated calomel electrode	92.1 % after 5000 cycles	S5
NiSe <sub>2</sub> nanosheet <sup>[6]</sup>	1M KOH	466 F g <sup>-1</sup> at 3 A g <sup>-1</sup>		Hg/HgO electrode	81.3 % after 1000 cycles	S6
NiCo <sub>2.1</sub> Se <sub>3.3</sub> /Graphene <sup>[7]</sup>	6M KOH	742.4 F g <sup>-1</sup> at 1 mA cm <sup>-2</sup>		Hg/HgO electrode	83.8 % after 1000 cycles	S7

CoSe <sub>2</sub> Nanoarrays <sup>[8]</sup>	3M KOH	759.5 F g <sup>-1</sup> at 1 mA cm <sup>-2</sup>	saturated calomel electrode	94.5 % after 5000 cycles	S8
Ni <sub>0.9</sub> Co <sub>1.92</sub> Se <sub>4</sub> <sup>[9]</sup>	3M KOH	1021.1 F g <sup>-1</sup> at 2 mA cm <sup>-2</sup>	Hg/HgO electrode	88.39 % after 5000 cycles	S9
Ni <sub>0.5</sub> Co <sub>0.5</sub> Se <sub>2</sub> <sup>[10]</sup>	6M KOH	524 C g <sup>-1</sup> at 1 A g <sup>-1</sup>	Hg/HgO electrode	91 % after 3500 cycles	S10
CoSe <sub>2</sub> /C <sup>[11]</sup>	2M KOH	726 F g <sup>-1</sup> at 2 A g <sup>-1</sup>	saturated calomel electrode	85.1 % after 2000 cycles	S11
NiCo <sub>2</sub> S <sub>2.2</sub> Se <sub>1.8</sub> /CC <sup>[12]</sup>	6M KOH	870 C g <sup>-1</sup> at 2.5 A g <sup>-1</sup>	Hg/HgO electrode	83 % after 5000 cycles	S12
NiSe nanorod <sup>[13]</sup>	6M KOH	6.81 F g <sup>-1</sup> at 5 mA cm <sup>-2</sup>	Hg/HgO electrode	78.9% after 2000 cycles	S13
NiSe <sub>2</sub> <sup>[14]</sup>	4 M KOH	1044 F g <sup>-1</sup> at 3 A g <sup>-1</sup>	Ag/AgCl electrode	67 % after 2000 cycles	S14
CoSe <sup>[15]</sup>	1M KOH	510 F g <sup>-1</sup> at 1 A g <sup>-1</sup>	saturated calomel electrode	91% after 5000 cycles	S15

## References

- [1] H. Chen, S. Chen, M. Fan, C. Li, D. Chen, G. Tian, K. Shu, *Journal of Materials Chemistry A* **2015**, 3, 23653.
- [2] H. Chen, M. Fan, C. Li, G. Tian, C. Lv, D. Chen, K. Shu, J. Jiang, *Journal of Power Sources* **2016**, 329, 314.
- [3] L. Quan, T. Liu, M. Yi, Q. Chen, D. Cai, H. Zhan, *Electrochimica Acta* **2018**, 281, 109.
- [4] X. Zhao, X. Li, Y. Zhao, Z. Su, Y. zhang, R. Wang, *Journal of Alloys and Compounds* **2017**, 697, 124.
- [5] L. Hou, Y. Shi, C. Wu, Y. Zhang, Y. Ma, X. Sun, J. Sun, X. Zhang, C. Yuan, *Advanced Functional Materials* **2018**, 28.
- [6] A. Chang, C. Zhang, Y. Yu, Y. Yu, B. Zhang, *ACS Appl Mater Interfaces* **2018**, 10, 41861.
- [7] Y. Wang, W. Zhang, X. Guo, K. Jin, Z. Chen, Y. Liu, L. Yin, L. Li, K. Yin, L. Sun, Y. Zhao, *ACS Appl Mater Interfaces* **2019**, 11, 7946.
- [8] T. Chen, S. Li, J. Wen, P. Gui, Y. Guo, C. Guan, J. Liu, G. Fang, *Small* **2018**, 14.
- [9] W. An, L. Liu, Y. Gao, Y. Liu, J. Liu, *RSC Advances* **2016**, 6, 75251.
- [10] X. Song, C. Huang, Y. Qin, H. Li, H. C. Chen, *Journal of Materials Chemistry A* **2018**, 6, 16205.
- [11] Y. Zhang, A. Pan, Y. Wang, X. Cao, Z. Zhou, T. Zhu, S. Liang, G. Cao, *Energy Storage Materials* **2017**, 8, 28.
- [12] J. Lin, Z. Zhong, H. Wang, X. Zheng, Y. Wang, J. Qi, J. Cao, W. Fei, Y. Huang,

- J. Feng, *Journal of Power Sources* **2018**, 407, 6.
- [13] Y. Tian, Y. Ruan, J. Zhang, Z. Yang, J. Jiang, C. Wang, *Electrochimica Acta* **2017**, 250, 327.
- [14] S. Wang, W. Li, L. Xin, M. Wu, Y. Long, H. Huang, X. Lou, *Chemical Engineering Journal* **2017**, 330, 1334.
- [15] X. Zhang, J. Gong, K. Zhang, W. Zhu, J.-C. Li, Q. Ding, *Journal of Alloys and Compounds* **2019**, 772, 25.